



Science Arts & Métiers (SAM)

is an open access repository that collects the work of Arts et Métiers Institute of Technology researchers and makes it freely available over the web where possible.

This is an author-deposited version published in: <https://sam.ensam.eu>
Handle ID: <http://hdl.handle.net/10985/15117>

To cite this version :

Guy CAIGNAERT, Geneviève DAUPHIN-TANGUY, Antoine DAZIN - Model based analysis of the time scales associated to pump start-ups - Nuclear Engineering and Design - Vol. 293, p.218-227 - 2015

Any correspondence concerning this service should be sent to the repository

Administrator : scienceouverte@ensam.eu



Model Based Analysis of the Time Scales associated to Pump Start-ups

Antoine Dazin¹, Guy Caignaert¹, Geneviève Dauphin-Tanguy²

⁽¹⁾ Arts et métiers ParisTech / LML Laboratory UMR CNRS 8107, 8 bld Louis XIV, 59046 Lille cedex, France

(33) 3 20 62 21 68, antoine.dazin@lille.ensam.fr

⁽²⁾ Univ Lille Nord de France, Ecole Centrale de Lille/ CRISTAL UMR CNRS 9189, BP 48, 59651 Villeneuve d'Ascq cedex., F 59000 France genevieve.dauphin-tanguy@ec-lille.fr

ABSTRACT

The paper refers to a non dimensional analysis of the behaviour of a hydraulic system during pump fast start-ups. The system is composed of a radial flow pump and its suction and delivery pipes. It is modelled using the bond graph methodology. The prediction of the model is validated by comparison to experimental results. An analysis of the time evolution of the terms acting on the total pump pressure is proposed. It allows for a decomposition of the start-up into three consecutive periods. The time scales associated with these periods are estimated. The effects of parameters (angular acceleration, final rotation speed, pipe length and resistance) affecting the start-up rapidity are then explored.

Keywords : Transient, Pump start-up, Bond-graph model, time scales.

Introduction

Cooling systems are a crucial point of nuclear power plants safety. Transient operations are commonly encountered in such hydraulic systems, (Gao et al 2013, Farhadi et al 2007) and an accurate prediction of their behavior during these operations is necessary. Nevertheless, the performance of their components during these transient periods is rather different than during the steady one. Concerning pumps, this has been well established, through different studies dealing with :

- Starting periods in non cavitating (Tsukamoto and Ohashi (1982), Saito (1982), Ghelici (1993), Bolpaire (2000), Lefebvre and Barker (1995)) or cavitating conditions (Tanaka & Tsukamoto (1999), Duplaa et al (2010, 2013).
- Stopping periods (Tsukamoto et al, (1986)),
- Valve opening and closure (Picavet, (1999) – Dazhuan et al (2010))

Quasi-steady models (using the steady performance of the pump) are still in use for the transient performance prediction of pumps during starting periods (Rizwan Uddin 1994). They give rather good results if the transient is relatively slow (i.e. if the transient effects are negligible compared with the steady one). However, to obtain reliable results compared with the experiments, in case of fast transient periods, more sophisticated models, including the effects due to the acceleration of the runner and of the flow, have been built (Tsukamoto et al (1982), Dazin et al (2007)).

Besides, whereas the similarity laws for steady operation of hydraulic turbomachineries are well established, very few works are dealing with the non dimensional analysis of a fast start-up. Tsukamoto et al (1982) have introduced the non-dimensional parameter $\omega_f T_{na}$ (where ω_f is the final rotation speed and T_{na} is a time characteristic of the start-up) as the most important parameter for the transient characteristics of a pump.

An attempt to determine which parameter are affecting the performance of a pump during a start-up has been proposed by Dazin et al (2006) through the study of experimental results: start-ups with various final operating points and acceleration were the support of an analysis of the performance of a pump operating in transient operations. Unfortunately, the analysis was limited because of some experimental constraints: the acceleration rate was not easily driven because the fast start-ups were obtained by an electromagnetic clutch which is not easy to control. It was also not possible to change the geometry of the test rig. On top of that, the relative uncertainty measurement is very high at the beginning of the start-up and the analysis of the results is thus difficult during the first period of the transient.

More recently, Elaoud et al (2011) have proposed a study based on the modelling of the governing equations of the transient flow in pipes to analyse the effect of pump starting times on the transient flow in pipes.

The purpose of the present work is to present a more universal analysis of pump start-ups. More precisely, it aims at giving the time scales associated to pumps start-up and to determine which parameters can affect them. To do so, a model of a whole hydraulic test rig has been simulated using the bond graph methodology.

The prediction of the model proposed in the present paper is validated by comparison to experimental data from Bolpaire (2000). An analysis of the evolution with time of the terms contained in the instantaneous total pressure increase in the pump is proposed using non dimensional results with a log-log presentation allowing for a clear decomposition of a start-up into three periods whose duration can be estimated. Then, this analysis is used to investigate the impact of the variation of several parameters (acceleration rate, final rotation speed, final flow rate, pipe lengths) on the intensity and duration of the transient effects during a start-up. These analyses are made assuming non cavitating operation conditions. It is also assumed that the pressure wave propagation phenomena within the system and the pump are neglected, as the paper focuses on the interpretation of the instantaneous pump performance.

1/ BOND GRAPH MODEL

11/ Presentation of the model

The test rig modelled (Fig. 1) is a closed loop composed of a radial flow pump connected to a tank (at atmospheric pressure) through hydraulic pipes. A valve is also available on the test rig, in order to set the final operating point. The whole system is modelled using the bond-graph methodology.

A bond graph consists of subsystems linked together by half arrows, representing power bonds. They exchange instantaneous power at places called ports. The variables that are forced to be identical when two ports are connected are the power variables, considered as functions of time. The various power variables are classified in a universal scheme, and called either effort $e(t)$ (force, torque, pressure, voltage, temperature...) or flow $f(t)$ (velocity, angular velocity, volume flow rate, current, entropy flow ...). Their product $P(t) = e(t).f(t)$ is the instantaneous power flowing between the ports. Two other types of variables, called energy variables, turn out to

be important in describing dynamic systems: the momentum $p(t) = \int e(t)dt$ and the displacement $q(t) = \int f(t)dt$ in generalized notation.

A few basic types of elements are required in order to represent models in a variety of energy domains. For 1D-system modelling, basic 1-port elements represent power dissipation (R), energy storage (I, C) and power supply (effort and flow sources), changing of domains without power losses (TF and GY-elements). A causal stroke, placed perpendicularly to the bond, shows up the way the constitutive relations in an element have to be written. The model bond graph can be directly simulated using software with a graphical bond graph interface, as 20Sim (Controllab Products) software used here. From the bond graph model can be derived dynamic mathematical models, under ODE (ordinary differential equation) or DAE (differential algebraic equation) equations, which can be simulated using software as Matlab/Simulink. Plenty of papers exist in the literature. For more details on this methodology, see for example Karnopp (1975).

Before describing the model, one can note that :

- all the pressures are expressed in terms of total pressure,
- as the flow is considered to be incompressible, the volume flow rate q is the same in all the components that will be described in the following.

The synoptic of the bond graph model is presented Fig. 2. It is composed of:

- An effort source (a constant pressure boundary condition) used to model the tank.
- A dissipative element (R) representing the hydraulic losses in the pipes and the valve. These losses are supposed to be proportional to the square of the volume flow rate.

$$\Delta P = \frac{1}{2} k \rho \left(\frac{q}{S} \right)^2 \quad (1)$$

Where ΔP are the total pressure losses in the pipe and the valve, q , the volume flow rate, ρ the fluid density, S the pipe cross-section area and k , the loss coefficient which is adjusted for each start-up in order to reach the desired final operating point (the adjustment of this parameter could be compared to the opening/closing of a valve to set an experimental operating point).

- An inertial element (I) representing the inertial hydraulic effects in the pipes and depending on the geometry of the pipe:

$$\Delta P = \rho \frac{L}{S} \frac{dq}{dt} \quad (2)$$

Where L is the total pipe length and S , the pipe cross-section area.

- The model of the pump is based on the one proposed by Dazin et al (2007) for radial flow pumps.

$$\Delta P_{pump} = \Delta P_s + \rho \left[K_\omega \frac{d\omega}{dt} - K_q \frac{dq}{dt} - \frac{L_d}{S_d} \frac{dq}{dt} - \frac{L_{vol}}{S_{vol}} \frac{dq}{dt} \right] \quad (3)$$

With:

ω , the instantaneous angular speed of the impeller,

ΔP_{pump} , the instantaneous pump total pressure rise,

ΔP_s a steady term representing the steady total pressure rise of the pump (i.e. the pressure rise obtained at a given velocity and flow rate in steady condition), supposed to be well described by the following polynomial approximation:

$$\frac{\rho \Delta P_s}{R_2^2 \omega^2} = a_1 \left(\frac{q}{R_2^3 \omega} \right)^2 + a_2 \frac{q}{R_2^3 \omega} + a_3 \quad (4)$$

L_d , A_d , L_{vol} and A_{vol} are the equivalent lengths and sections of the diffuser and volute of the pump, and are used to estimate the hydraulic inertial effects in the pump stator.

$K_\omega = \int_{R_1}^{R_2} \frac{r dr}{\tan \beta(r)}$, a parameter which allows estimating the impact of the angular acceleration effects on the pump instantaneous total pressure rise.

$K_q = \frac{1}{4\pi} \int_{R_1}^{R_2} \frac{dr}{r \cdot b(r) \cdot \sin^2(\beta(r))}$, a parameter which allows estimating the impact of the fluid inertia in the impeller on the pump instantaneous total pressure rise.

In this two expressions, R_1 and R_2 are the inlet and outlet radii of the impeller, b the height of the blade passage and β is the relative flow angle.

These steady and angular acceleration terms are modelled by a gyrator (MGY). The hydraulic inertial effects in the rotor and in the stator (diffuser and volute) are modelled separately by two inertial elements.

Table 1: Pump specifications

Impeller geometric specifications		Diffuser geometric specifications		Hydraulic Specifications	
Inlet vane angle $\beta_{1\alpha}$	32.2°	Inlet Diameter R_3	101.5 mm	Nominal speed	2900 rpm
Outlet vane angle $\beta_{2\alpha}$	23°	Outlet Diameter R_4	120 mm	Nominal flow rate	23 m³/h
Number of vanes	5	Constant width b_3	6 mm	Nominal total pump pressure	4.15 bar
Inlet diameter R_1	19.25 mm				
Outer diameter R_2	101.25 mm				
Outer width b_2	7 mm				

The angular velocity evolution is imposed to the pump through a modulated flow source (MSf). This evolution is obtained with a first order transfer function whose equation is given by $\frac{\kappa}{s+\tau}$, where κ is the gain, τ , the time constant and s , the complex Laplace variable. In this function, the gain and time constant are set in order to fix the final angular velocity and start-up duration.

The integration method used to solve the equations system is a backward differentiation formula.

The geometrical parameters needed to model the pump are calculated using the geometry of the single volute radial flow pump used in the experiments realised by Bolpaire (2000) and reported by Dazin et al (2007). The main geometrical characteristics of this pump are reminded in Table 1.

12/ Experimental validation

To check the validity of this model, its results are compared with experimental ones. To do so, the angular velocity input is replaced by an experimental velocity evolution (Fig.3a) extracted from Bolpaire (2000). The pipe length and section are adjusted to reproduce the experimental test rig. The loss coefficient of the valve is adjusted to reach the final experimental operating point. The experimental evolution of the pump total pressure rise is compared with the evolution predicted by the model Fig. 3b. The differences between the experimental and model data are less than 1% during the first part of the start-up ($t < 0.2$ s) and are never exceeding 7%. This confirms the validity of the model (this validity has already been established in Dazin et al (2007) for a single pump model, but not for a complete loop).

13/ SIMULATION TEST PLAN

The test cases are summarized in Table 2. The first case (a reference case) corresponds to a start-up for which the final operating point corresponds to the pump nominal point. The time constant of the first order filter is set to $\tau = 0.2$ s. The pipe length is set to $L = 5$ m whereas the pipe diameter is 0.04 m. The second, third and fourth cases correspond to variation of the final steady operating point (final velocity for case 2 and final flow rate for cases 3 and 4), compared with the first case. Cases 5 and 6 correspond to start-ups ending at the same operating point as case 1 but with different acceleration rates. Case 7 corresponds to a variation of the pipe lengths ($L = 10$ m instead of 5 m). The pipe diameter is remained unchanged whatever the case considered is.

Table 2: Test plan

	Final speed (rpm)	Final flow rate (m³/h)	Pressure loss coefficient k	Time constant	Pipe
1	2900	23 (q_n)	33.2	$\tau=0.2$ s	Short ($L = 5$ m)
2	1450	11.5 (q_n)	33.2	$\tau=0.2$ s	Short ($L = 5$ m)
3	2900	34.5 (1.5 q_n)	10	$\tau=0.2$ s	Short ($L = 5$ m)
4	2900	11.5 (0.5 q_n)	157	$\tau=0.2$ s	Short ($L = 5$ m)
5	2900	23 (q_n)	33.2	$\tau=2$ s	Short ($L = 5$ m)
6	2900	23 (q_n)	33.2	$\tau=20$ s	Short ($L = 5$ m)
7	2900	23 (q_n)	33.2	$\tau=0.2$ s	Long ($L = 10$ m)

2/ REFERENCE CASE – TIME SCALES ASSOCIATED TO A START-UP

Fig. 4 presents typical simulation results for the reference case (case 1 in table 2). These are typical results obtained for a fast start-up. The acceleration rate is relatively high (it takes 0.32 s to reach 80% of the final impeller angular speed).

The pressure and flow rate are rising with a lag due to inertial effects in the pump and pipes. Fig 5 shows what can be the interest of using log log scale to present such results : the flow rate and the pump rotation speed are normalized by their final values in steady operating conditions and time is normalized by τ : as expected, the

evolution of the velocity is linear as it is imposed by the first order filter ; but it is also very clear on fig 5, that the evolution of the flow rate is proportional to t^3 during a large part of the start-up. This evolution will be explained in the next paragraphs of the present paper.

The comparison of the steady non dimensional characteristics $\left(\psi = \frac{\Delta P}{\rho \omega^2 R_2^2}, \delta = \frac{q}{R_2^3 \omega} \right)$ of the pump and of the non dimensional characteristics of the start-up is proposed in Fig 6. It is very similar to the ones observed experimentally (Tsukamoto et Ohashi (1982), Saito (1982), Lefebvre et Baker (1995)). Two phenomena can be identified. At the beginning of the start-up, the pressure coefficient is higher than the steady one because of angular acceleration effect. In a second stage, the pressure coefficient is lower than the steady one, because of inertial effects in the pump. At the end of the start-up, the pump is reaching its final (steady) operating point.

The time evolutions of several pressure coefficients are presented in Fig. 7. On this figure can be found:

- $\psi_{pump} = \frac{\Delta P_{pump}}{\rho \omega^2 R_2^2}$, the instantaneous total pressure coefficient of the pump.

- $\psi_s = \frac{\Delta P_s}{\rho \omega^2 R_2^2}$: the steady term that seems to be nearly constant during a great part of the start-up. This is due to the fact that the flow coefficient remains at a very low value while t/τ is lower than 10^{-1} (Fig. 8) because the angular velocity of the runner is increasing more rapidly than the volume flow rate (Fig. 5). The pump is then operating in the left part ($\delta < 0.001$) of its steady characteristics curve where the pressure coefficient is nearly constant.

- $\psi_\omega = \frac{K_\omega \frac{d\omega}{dt}}{\rho \omega^2 R_2^2}$: the acceleration effects on the pump performance. It is the dominant term at the very beginning of the start-up because the acceleration rate is great and the velocity is low. It can be noticed that the evolution of this parameter is quasi-linear when plotted in a log-log scale (with a slope equal to -2). This is due to the fact that the impeller acceleration is nearly constant during a great part of the start-up. Thus, the pressure coefficient time-evolution is proportional to ω^{-2} , that is to t^{-2} .

As the velocity increases rapidly, this term decreases rapidly and becomes negligible for $t^* > 0.01$.

- $\psi_{q_imp} = \frac{K_q \frac{dq}{dt}}{\rho \omega^2 R_2^2}$, $\psi_{q_stator} = \frac{\left(\frac{L_d}{S_d} + \frac{L_{vol}}{S_{vol}} \right) \frac{dq}{dt}}{\rho \omega^2 R_2^2}$: the inertial terms in the impeller and in the pump stator.

They are quite important during a great part of the start-up. It can also be noticed that, because of the geometry of the pump studied, the inertial effects are greater in the stator (diffuser and volute) than in the rotor. At the beginning of the start-up ($t^* < 0.01$), these terms are also proportional to t^{-2} . This can be explained easily from the equations governing the system. The one governing the pipes can be written as follows:

$$\Delta P_{pipe} = K q^2 + \rho \frac{L}{S} \frac{dq}{dt} \quad (5a)$$

$$\text{Where } K = \frac{1}{2} \frac{\rho k}{S^2}$$

Which gives, in a dimensionless form :

$$\frac{\Delta P_{pipe}}{\rho \omega^2 R_2^2} = \frac{K q^2}{\rho \omega^2 R_2^2} + \frac{1}{\omega^2 R_2^2} \frac{L}{S} \frac{dq}{dt} \quad (5b)$$

It can be noticed that the pressure delivered by the pump ΔP_{pump} is equal to the pressure ΔP_{pipe} required by the system. Consequently, combining equation (3) and (5) gives :

$$\Delta P_s = K q^2 + \rho \frac{L}{S} \frac{dq}{dt} - \rho \left[K_\omega \frac{d\omega}{dt} - K_q \frac{dq}{dt} - \frac{L_d}{S_d} \frac{dq}{dt} - \frac{L_{vol}}{S_{vol}} \frac{dq}{dt} \right] \quad (6a)$$

Which gives, in a dimensionless form :

$$\psi_s + \psi_\omega = \psi_{losses} + \psi_{q_pipe} + \psi_{q_imp} + \psi_{q_stator} \quad (6b)$$

Where $\psi_{losses} = \frac{Kq^2}{\rho\omega^2 R_2^2}$, and represents the non-dimensional pressure losses in the pipes and in the valve, and

ψ_{q_pipe} represents the dimensionless hydraulic inertial effects in the pipe.

At the beginning of the start-up, as pointed out above, the dominant term of this equation is the angular acceleration term. More precisely, the steady term ΔP_s is negligible (see Fig. 7). The resistive term is also negligible because the flow rate is very low at the beginning of the start-up. Finally, equation (6a) becomes:

$$K_\omega \frac{d\omega}{dt} \approx \left[\frac{L}{S} + K_q + \frac{L_d}{S_d} + \frac{L_{vol}}{S_{vol}} \right] \frac{dq}{dt} \quad (7)$$

This proves that, at the beginning of the start-up, the evolution of the flow acceleration is proportional to the angular acceleration.

In a second time period (from $t^* = 0.01$ to $t^* = 1$), the two terms $\psi_{q_imp} = \frac{K_q \frac{dq}{dt}}{\rho\omega^2 R_2^2}$ and $\psi_{q_stator} = \frac{(\frac{L_d}{S_d} + \frac{L_{vol}}{S_{vol}}) \frac{dq}{dt}}{\rho\omega^2 R_2^2}$ appear to be nearly constant. This can also be explained through the analysis of equation (6): as pointed out above, in this equation, the angular acceleration term is negligible when $t^* > 0.01$. Besides, the first term of the right hand side of equation (6a & b), that is the resistive term, is also negligible from $t^* = 0.01$ to $t^* = 1$ because the flow rate is still very low.

Consequently, from $t^* = 0.01$ to $t^* = 1$, equation (6) can be written:

$$\psi_s \approx \rho \left[\frac{L}{S} + K_q + \frac{L_d}{S_d} + \frac{L_{vol}}{S_{vol}} \right] \frac{dq/dt}{\rho R_2^2 \omega^2}. \quad (8)$$

As the steady pressure coefficient is constant during the beginning of the start-up, the term $\frac{dq/dt}{\rho R_2^2 \omega^2}$ is also constant while the resistive effects in the test rig are negligible compared to the resistive effect in the pipe.

Consequently, $\frac{dq}{dt}$ is proportional to t^2 . This explains why the flow rate q is proportional to t^3 (as observed Fig. 6.)

Finally, the start-up of a pump can be decomposed into three periods.

First period: During the very beginning of the start-up ($t^* < 0.01$ on Fig 7) the dominant effects are the angular acceleration effects in the pump. During this period, the flow acceleration is proportional to the angular acceleration. It can be said that in this first period, the start-up is governed by the motor and the driving shaft characteristics.

$$\text{This period lasts as long as } \Delta P_s \ll \rho K_\omega \frac{d\omega}{dt} \text{ i.e. } \psi_s \ll \frac{K_\omega \frac{d\omega}{dt}}{\omega^2 R_2^2} \quad (9)$$

The order of magnitude of ψ_s is 1.

The order of magnitude of K_ω is $K_\omega \approx \frac{R_2^2}{\tan \beta_m}$, where β_m is the mean value of the relative flow angle in the impeller, defined as the average of the outlet and inlet relative flow angle.

The order of magnitude of $\frac{d\omega}{dt}$ is $\frac{\omega_f}{\tau}$, where ω_f is the final speed of the impeller. And consequently, the order of magnitude of the instantaneous speed is $\omega \approx \frac{\omega_f}{\tau} t$.

Consequently, the first period of the start-up ends at a normalised time t_1^* defined as follows:

$$t_1^* = \frac{t_1}{\tau} \approx \sqrt{\frac{1}{\tan \beta_m \omega_f \tau}} \quad (10)$$

It can be noticed that, in the previous expression, τ can be replaced by another time characteristic of the start-up. Thus, in the expression of t_1^* , the non-dimensional parameter $\omega_f \tau$ introduced by Tsukamoto et al (1982) as a parameter characteristic of the start-up, can be identified.

For the first case of table 2, and using the expression of equation (10), one obtain $t_1^* \approx 0.01$, which matches very well with the duration of the first period observed in Fig. 7.

Second period: In the second period ($0.01 < t^* < 1$), the start up is governed by the inertial effects in the test rig. During that period the flow rate is evolving as t^3 if the acceleration of the impeller is constant. This period lasts as long as the inertial effects in the loop are greater than the resistive effects in the pipes, i.e. as long as $\frac{L_{eq}}{S} \frac{dq}{dt} \gg \frac{1}{2} \rho k \left(\frac{q}{S}\right)^2$, where L_{eq} is the equivalent length of the whole loop and is defined as :

$$\frac{L_{eq}}{S} = \frac{L}{S} + K_q + \frac{L_d}{S_d} + \frac{L_{vol}}{S_{vol}}$$

During this time period, $\frac{L_{eq}}{S} \frac{dq}{dt} \approx R_2^2 \omega^2 \approx R_2^2 \frac{\omega_f^2}{\tau^2} t^2$

And consequently $q \approx \frac{1}{3} \frac{S}{L_{eq}} R_2^2 \frac{\omega_f^2}{\tau^2} t^3$, and so: $\frac{1}{2} k \left(\frac{q}{S}\right)^2 \approx \frac{1}{18} k \frac{R_2^4}{L_{eq}^2} \frac{\omega_f^4}{\tau^4} t^6$.

Consequently, the second period ends at a normalized time t_2^*

$$t_2^* = \frac{t_2}{\tau} \approx \left(\frac{18}{k}\right)^{\frac{1}{4}} \sqrt{\frac{L_{eq}}{R_2} \frac{1}{\omega_f \tau}} \quad (11)$$

In the present case (first case of table 2), and using the expression of equation (11), one obtain $t_2^* \approx 1.3$. It can be noticed that these value gives the correct order of magnitude of the observed time duration of the second time period which was estimated to be around 1 by the observation of Fig 7.

Third period: At last, in a third period, the resistive effects in the pipes are increasing and the start up tends to a quasi steady start –up.

Using the analysis of the pressure coefficients evolution, the impact of the parameters having an influence on the start-up is easier, and is illustrated by the simulation of cases 2 to 7 in the following section.

3/ PARAMETERS AFFECTING THE START-UP

31/ Effects of the acceleration rate and final speed

To compare the effect of the acceleration rate on the start-up, the evolution of ψ_ω (fig 9a), ψ_{q_imp} (fig 9b) and ψ_{pump} (fig 9c) are plotted for three different test cases :

- The reference test case for which the acceleration time is short ($\tau = 0.2$ s),
- test case 5, for which the acceleration time is moderate ($\tau = 2$ s),
- test case 6, for which the acceleration time is long ($\tau = 20$ s).

It appears that, as expected, an increase of the acceleration rate (i.e. a decrease of the time constant τ) leads to an increase of the pressure coefficient ψ_ω (Fig. 9a). It can also be observed (fig 9b and 9c) that the durations of the

first and second periods of the start-up are increased. This is consistent with the definition of the normalized times t_1^* and t_2^* introduced in equations (10) and (11): a decrease of τ leads to an increase of the duration of the first and second periods.

The evolution of ψ_ω (fig 10a), ψ_{q_imp} (fig 10b) and ψ_{pump} (fig 10c) is now plotted for two different rotation speeds (2900 rpm and 1450 rpm).

The effect of a diminution of the final speed (Fig. 10) is similar to the effect of an increase of the acceleration rate of the angular velocity as the parameters τ and ω_f play similar roles in equations (10) and (11).

32/ Effect of the pipe length and resistance

The evolution of ψ_ω (fig 11a), ψ_{q_imp} (fig 11b) and ψ_{pump} (fig 11c) is now plotted for 2 different pipe lengths. As the angular acceleration is imposed, there is no influence of the pipe length: the angular acceleration coefficient pressure coefficient ψ_ω is similar in both cases (fig 11a). On the contrary the hydraulic inertia pressure coefficients are plotted Fig.11b. This term is obviously smaller when longer pipes are used. This is well explained by equations (7) and (8) showing that longer pipes lead to a decrease of the time derivative of the flow rate. On the contrary, the duration of the second time period increases when the pipe length is higher, which is coherent with the definition of t_2^* (Equation 11).

A change of the pipe resistance has also been tested. To do so, the pressure loss coefficient k of the pipes has been changed. It has been adjusted to reach the design flow rate of the pump for the reference case, $0.5 q_n$ for case 3 of table 2 and $1.5 q_n$ for case 4 of table 2. It corresponds to what would have been obtained in an experimental test-rig by opening or closing of a valve.

The evolution of ψ_ω (fig 12a), ψ_{q_imp} (fig 12b) and ψ_{pump} (fig 12c) is now plotted for 3 final flow rates (and consequently, three values of the pipe loss coefficient. It does not affect at all the beginning of the start-up as it can be seen Fig. 12. The angular acceleration coefficient is not affected by the final flow rate because the angular acceleration is imposed in the model. The flow acceleration is also not affected by the resistance of the pipe during the second time period ($t^* < 1$) as the viscous effects are negligible during this period. Besides, this second time period is shorter when the final flow rate is greater, which is coherent with the estimation of the duration t_2^* , showing an increase when the loss coefficient is smaller.

CONCLUSION

In the present contribution, a detailed analysis of the start-up of a hydraulic system composed of a radial flow pump and its suction and delivery pipes is proposed. It is based upon simulations obtained using the bond-graph methodology.

The analysis of the results shows that the start-up of the pump can be decomposed into three main periods :

- In the first period, the effects of the angular acceleration are the dominant ones. During this phase, the flow acceleration is proportional to the angular acceleration. The order of magnitude of this stage duration is $t_1^* = \frac{t_1}{\tau} \approx \sqrt{\frac{1}{\tan\beta_m \cdot \omega_f \cdot \tau}}$.
- In the second period, the angular acceleration effects become negligible and the hydraulic inertial effects are dominant compared with the viscous effects. During this second period, the parameter

$\frac{1}{\omega^2} \frac{dq}{dt}$ is constant and consequently the flow rate is proportional to t^3 , if the acceleration rate of

the runner is constant. This second time period ends at $t_2^* = \frac{t_2}{\tau} \approx \left(\frac{18}{k}\right)^{\frac{1}{4}} \sqrt{\frac{L_{eq}}{R_2} \frac{1}{\omega_f \tau}}$.

- In the third period the viscous effects become dominant and the start-up is quasi-steady.

Consequently, concerning pump transient modelling it can be said that a quasi-steady simulation of a pump start-up is sufficient:

- for the simulation third period identified above.

-for the whole simulation if the two first periods identified above are short (i.e. if t_1^* and t_2^* are very small compared with 1). This happens when $\omega_f \tau$ is great.

Besides, an analysis of the variation of several parameters is proposed.

An increase of the acceleration rate or a decrease of the final speed have similar effects. They lead to an increase of the transient effect as well as an increase of the duration of the two first periods of the start-up described above.

An increase of the pipe length leads to an increase of the duration of the second period of the start-up as well as a decrease of the inertial effects amplitude.

At last, an increase of the losses in the pipe does not affect the amplitude of the transient effects but leads to a decrease of the duration of the second period of the transient period.

Nomenclature

Roman Letters

a_1, a_2, a_3 : coefficients of the polynomial expression approximating the steady performance curve (-)

b : width (m)

b_2 : impeller outlet width (m)

b_3 : diffuser width (m)

k : loss coefficient (-)

$K = \frac{1}{2} \frac{\rho k}{S^2}$: loss parameter (kg.m^{-7})

$K_q = \frac{1}{4\pi} \int_{R_1}^{R_2} \frac{dr}{r \cdot b(r) \cdot \sin^2(\beta(r))}$: impeller hydraulic inertia (m^{-1})

$K_\omega = \int_{R_1}^{R_2} \frac{r dr}{\tan \beta(r)}$: angular acceleration parameter (m^2)

L : pipe length (m)

L_d : diffuser equivalent length (m)

L_{eq} : equivalent length of the whole loop (m)

L_{vol} : volute equivalent length (m)

q : volume flow rate (m^3/s)

R_1 : impeller inlet radius (m)

R_2 : impeller outlet radius (m)

R_3 : diffuser inlet radius (m)

R_4 : diffuser outlet radius (m)

t : time (s)

$t^*=t/\tau$: dimensionless time (-)

t_1^* : dimensionless duration of the first period of the start-up (-)

t_2^* : dimensionless duration of the second period of the start-up (-)

T_{na} : time characteristic of the start-up (as define Tsukamoto & Ohashi 1982) (s)

S : pipe cross section area (m²)

S_d : diffuser equivalent cross section area (m²)

S_{vol} : volute equivalent cross section area (m²)

Greek Letters

β : flow angle (°)

$\beta_{1\alpha}$: inlet vane angle (°)

$\beta_{2\alpha}$: outlet vane angle (°)

β_m : mean value of the relative flow angle in the impeller (°)

$\delta = \frac{q}{R_2^3 \omega}$: flow coefficient (-)

$\Delta P = \frac{\Delta P}{\rho \omega^2 R_2^2}$: pressure difference (Pa)

ΔP_{pump} : total pressure delivered by the pump (Pa)

ΔP_{pipe} : total pressure required by the pipe (Pa)

ΔP_s : total steady pressure delivered by the pump (Pa)

κ : gain (-)

ψ : pressure coefficient (-)

$\psi_{losses} = \frac{K q^2}{\rho \omega^2 R_2^2}$: pressure coefficient representing the total pressure losses in the pipes and valve (-)

$\psi_{pump} = \frac{\Delta P_{pump}}{\rho \omega^2 R_2^2}$: total pressure coefficient of the pump (-)

$\psi_{q_imp} = \frac{K_q \frac{dq}{dt}}{\rho \omega^2 R_2^2}$: pressure coefficient representing the inertial effects in the impeller (-)

$\psi_{q_stator} = \frac{(\frac{L_d}{S_d} + \frac{L_{vol}}{S_{vol}}) \frac{dq}{dt}}{\rho \omega^2 R_2^2}$: pressure coefficient representing the inertial effects in the stator (-)

$\psi_{q_pipe} = \frac{(\frac{L}{S}) \frac{dq}{dt}}{\rho \omega^2 R_2^2}$: pressure coefficient representing the inertial effects in the pipes (-)

$\psi_s = \frac{\Delta P_s}{\rho \omega^2 R_2^2}$: steady total pressure coefficient of the pump (-)

$\psi_\omega = \frac{K_\omega \frac{d\omega}{dt}}{\rho \omega^2 R_2^2}$: pressure coefficient representing the acceleration effect in the pump (-)

ρ : fluid density (kg/m³)

τ : time constant characteristic of the start-up (s)

ω : angular speed (rad/s)

ω_f : final angular speed (rad/s)

References

- Bolpaire S. (2000)** : Etude des écoulements instationnaires dans une pompe en régime de démarrage ou en régime établi. PhD Thesis. Ecole Nationale Supérieure des Arts et Métiers. Lille. France.
- Dazin A, Coutier-Delgosha O., Caignaert G, Bois G. (2006)** Dimensionless analysis of a centrifugal pump during fast starting periods. 23rd IAHR Symposium – Yokohama-October 2006
- Dazin A., Caignaert G., Bois G. (2007)**, Transient behaviour of turbomachineries : Applications to radial flow pump start-ups. Journal of Fluids engineering, 129, 1436-1444,
- Dazhuan W., Peng W., Zhifeng L., Legin W. (2010)**. The transient flow in a centrifugal pump during the discharge valve rapid opening process. Nuclear Engineering and Design. 240, 4061-4068
- Duplaa S., Coutier-Delgosha O, Dazin A, Roussette O., Bois G., Caignaert G., (2010)** Experimental Study of a Cavitating Centrifugal Pump During Fast Startups, Journal. of Fluids Engineering. -, 132,
- Duplaa S, Coutier-Delgosha O., Dazin A., Bois G..** X-Ray Measurements in a Cavitating Centrifugal Pump During Fast Start-Ups. Journal of Fluids Engineering. – 135 (4)
- Elaoud S., Hadj-Taïeb Ezzedine (2011)** Influence of pump starting times on transient flow pipes. Nuclear Engineering and Design. 241, 3624-3631
- Farhadi K., Bousbia-salah A., D'Auria F., (2007)** A model for analysis of pump start-up transients in Tehran Research Reactor. Progress in Nuclear Energy. 49, 499-510.
- Gao H., Gao F., Zhao X., Chen J., Cao X. (2013)**, Analysis of reactor coolant pump transient performance in primary coolant system during start-up period. Annals of Nuclear Energy 54. 202 – 208.
- Ghelici N. (1993)**, Etude du régime transitoire de démarrage rapide d'une pompe centrifuge, PhD Thesis. Ecole Nationale Supérieure d'Arts et Métiers - Lille, France.
- Karnopp D.C., Rosenberg R.C., Systems dynamics : a unified approach, John Wiley and son, 1975.**
- Lefebvre P. J., Barker W. P. (1995)** Centrifugal Pump Performance During Transient Operation, Journal of Fluids Engineering, vol. 117, pp 123 – 128
- Picavet A. (1996)**, Etude des phénomènes hydrauliques transitoires lors du démarrage rapide d'une pompe centrifuge, PhD Thesis. Ecole Nationale Supérieure des Arts et Métiers.
- Rizwan-Uddin (1994)** Steady-state characteristics based model for centrifugal pump transient analysis. Ann. Nucl. Energy. 21(5), 321-324
- Saito S. (1982)** The Transient Characteristics of a Pump During Start Up, Bulletin of JSME, vol. 25, n° 201, paper n°201-10, pp. 372 – 379
- Tanaka T., H. Tsukamoto (1999)**, Transient behaviour of a cavitating centrifugal pump at rapid change in operating conditions—Part 2: Transient phenomena at pump Start-up/Shutdown. Journal of Fluids Engineering, 121, 850-856.
- Tsukamoto H., Ohashi H., (1982)** Transient Characteristics of a Centrifugal Pump During Starting Period, Journal of Fluids Engineering. Transactions of ASME, vol. 104, pp. 6 – 14
- Tsukamoto H, Matsunaga S, Yoneda H (1986)**, Transient characteristics of a centrifugal pump during stopping period. ASME Journal of Fluid Engineering, 108(4): 392-399, 1986.

FIGURE CAPTIONS :

Figure 1 : Sketch of the hydraulic test rig

Figure 2: Synoptic of the bond graph model.

Figure 3 : Time evolution of the experimental angular velocity (a) and comparison of the pressure evolution (b)

Figure 4 : Time evolution of the angular velocity, volume flow rate pressure of the pump.

Figure 5 : Time-evolutions of the pump angular velocity and of the flow rate (log-log representation).

Figure 6 : a. Pump pressure coefficient as a function of the pump flow coefficient during the start-up (in blue) compared with the pump steady characteristics (in red). b. zoom on the initial instants of the start-up.

Figure 7: Time evolution of several pressure coefficients in a Log-log presentation.

Figure 8: Time evolution of the flow coefficient.

Figure 9: Comparison of the pressure coefficient evolution for three acceleration rates (cases 1, 5 and 6 of table 2)

Figure 10 : Comparison of the pressure coefficient evolution for 2 final speeds (cases 1 and 2 from table 2)

Figure 11 : Comparison of the pressure coefficients for two different pipe lengths (cases 1 and 7 from table 2).

Figure 12 : Effect of the pipe resistance (and consequently of the final flow rate -case 1, 3 and 4 from table 2)

References

- Bolpaire S. (2000)** : Etude des écoulements instationnaires dans une pompe en régime de démarrage ou en régime établi. PhD Thesis. Ecole Nationale Supérieure des Arts et Métiers. Lille. France.
- Dazin A, Coutier-Delgosha O., Caignaert G, Bois G. (2006)** Dimensionless analysis of a centrifugal pump during fast starting periods. 23rd IAHR Symposium – Yokohama-October 2006
- Dazin A., Caignaert G., Bois G. (2007)**, Transient behaviour of turbomachineries : Applications to radial flow pump start-ups. Journal of Fluids engineering, 129, 1436-1444,
- Dazhuan W., Peng W., Zhifeng L., Leqin W. (2010)**. The transient flow in a centrifugal pump during the discharge valve rapid opening process. Nuclear Engineering and Design. 240, 4061-4068
- Duplaa S., Coutier-Delgosha O, Dazin A, Roussette O., Bois G., Caignaert G., (2010)** Experimental Study of a Cavitating Centrifugal Pump During Fast Startups, Journal. of Fluids Engineering. -, 132,
- Duplaa S, Coutier-Delgosha O., Dazin A., Bois G.** X-Ray Measurements in a Cavitating Centrifugal Pump During Fast Start-Ups. Journal of Fluids Engineering. – 135 (4)
- Elaoud S., Hadj-Taïeb Ezzedine (2011)** Influence of pump starting times on transient flow pipes. Nuclear Engineering and Design. 241, 3624-3631
- Farhadi K., Bousbia-salah A., D'Auria F., (2007)** A model for analysis of pump start-up transients in Tehran Research Reactor. Progress in Nuclear Energy. 49, 499-510.
- Gao H., Gao F., Zhao X., Chen J., Cao X. (2013)**, Analysis of reactor coolant pump transient performance in primary coolant system during start-up period. Annals of Nuclear Energy 54. 202 – 208.
- Ghelifci N. (1993)**, Etude du régime transitoire de démarrage rapide d'une pompe centrifuge, PhD Thesis. Ecole Nationale Supérieure d'Arts et Métiers - Lille, France.
- Karnopp D.C., Rosenberg R.C., Systems dynamics : a unified approach, John Wiley and son, 1975.**
- Lefebvre P. J., Barker W. P. (1995)** Centrifugal Pump Performance During Transient Operation, Journal of Fluids Engineering, vol. 117, pp 123 – 128
- Picavet A. (1996)**, Etude des phénomènes hydrauliques transitoires lors du démarrage rapide d'une pompe centrifuge, PhD Thesis. Ecole Nationale Supérieure des Arts et Métiers.
- Rizwan-Uddin (1994)** Steady-state characteristics based model for centrifugal pump transient analysis. Ann. Nucl. Energy. 21(5), 321-324
- Saito S. (1982)** The Transient Characteristics of a Pump During Start Up, Bulletin of JSME, vol. 25, n° 201, paper n°201-10, pp. 372 – 379
- Tanaka T., H. Tsukamoto (1999)**, Transient behaviour of a cavitating centrifugal pump at rapid change in operating conditions—Part 2: Transient phenomena at pump Start-up/Shutdown. Journal of Fluids Engineering, 121, 850-856.
- Tsukamoto H., Ohashi H., (1982)** Transient Characteristics of a Centrifugal Pump During Starting Period, Journal of Fluids Engineering. Transactions of ASME, vol. 104, pp. 6 – 14
- Tsukamoto H, Matsunaga S, Yoneda H (1986)**, Transient characteristics of a centrifugal pump during stopping period. ASME Journal of Fluid Engineering, 108(4): 392-399, 1986.

Figure1

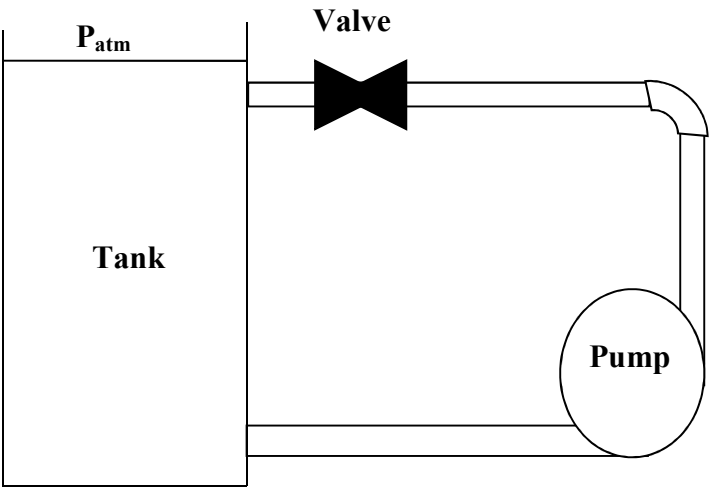


Figure2

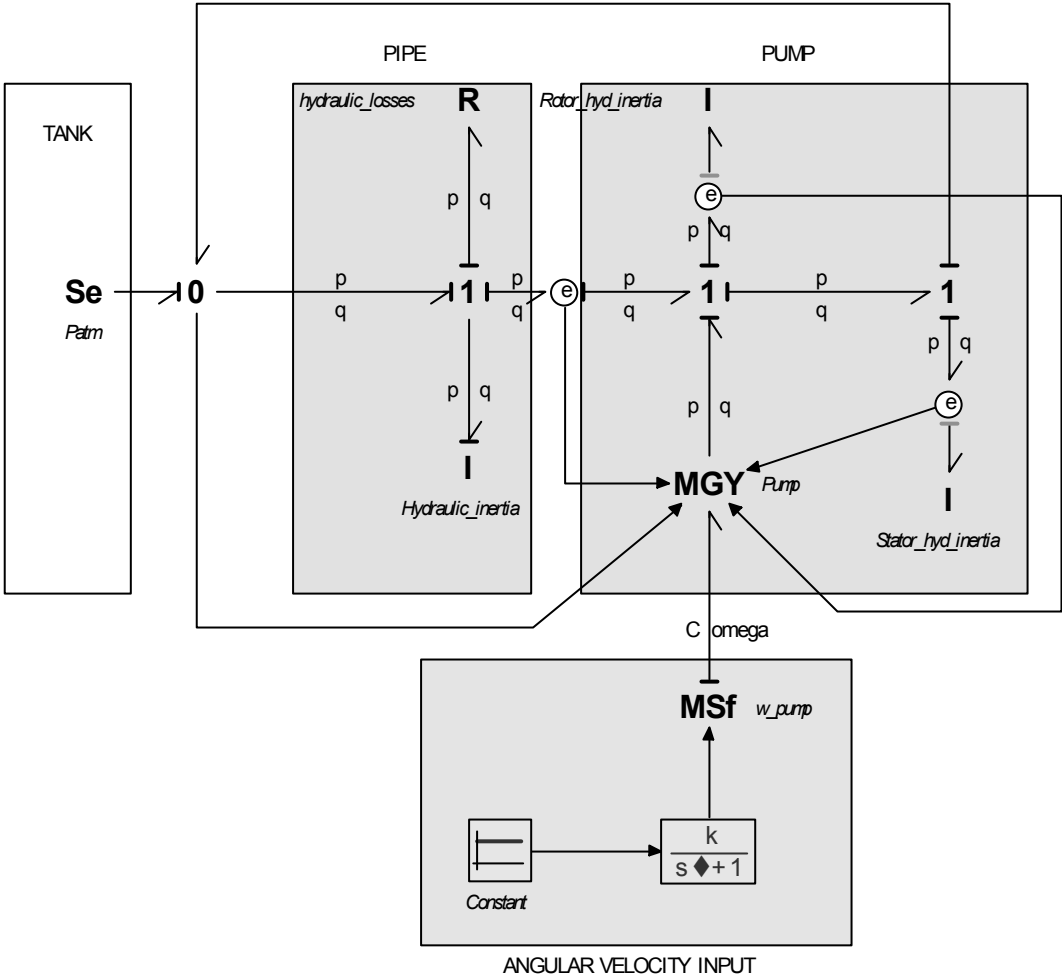


Figure3a

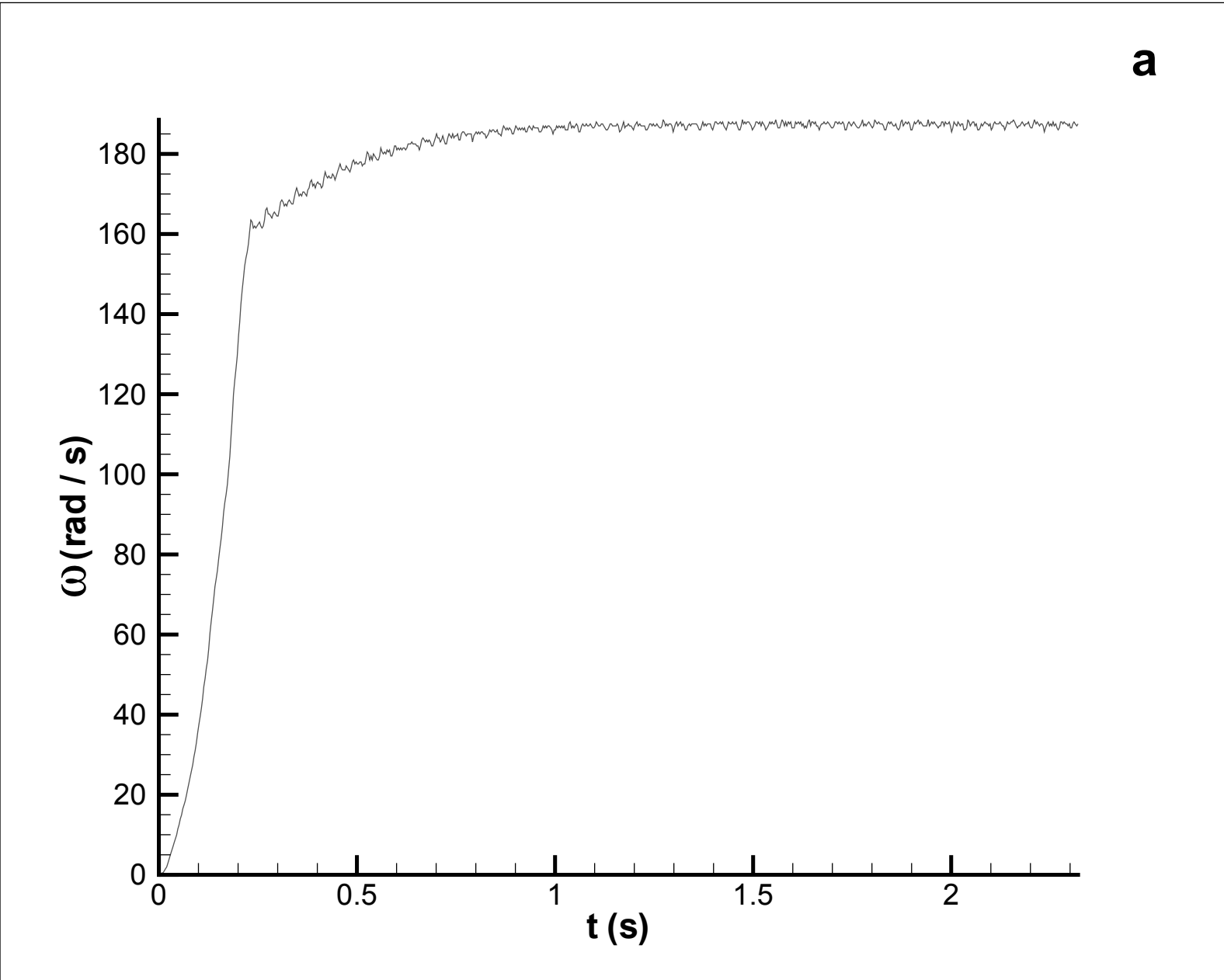
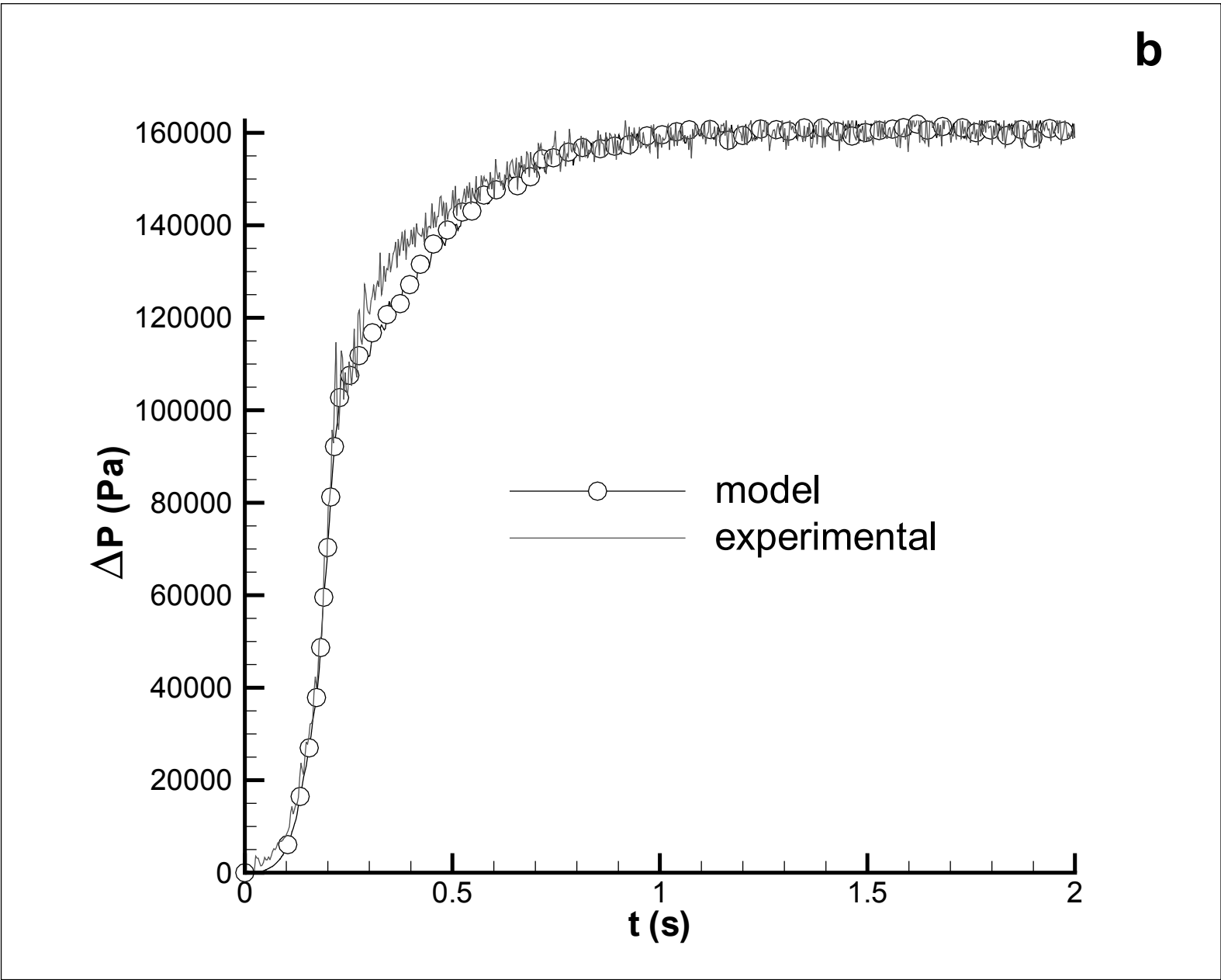


Figure3b



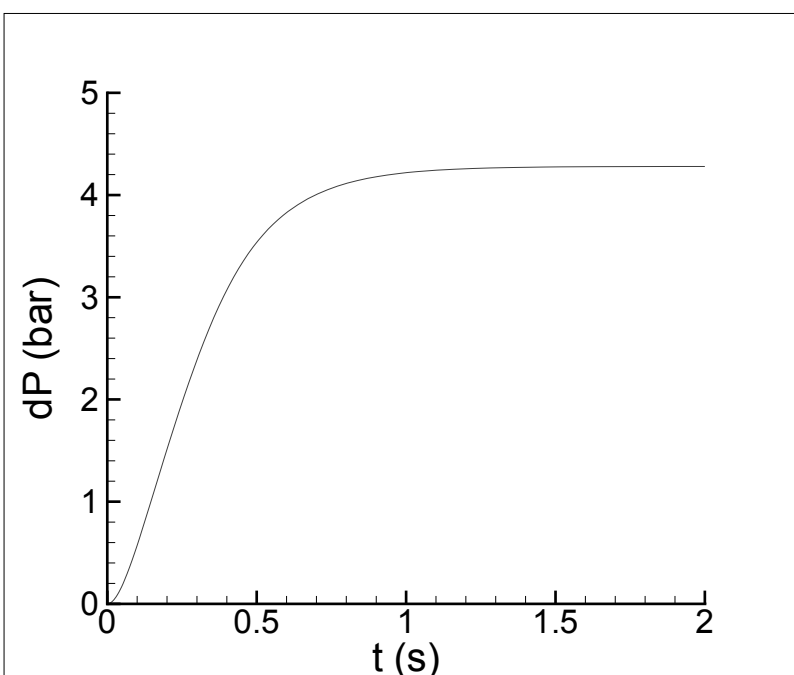
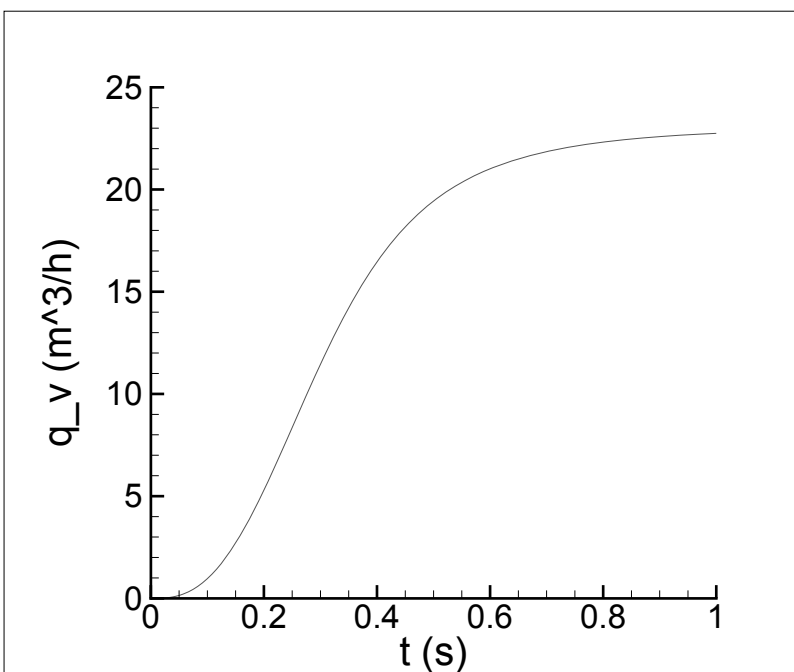
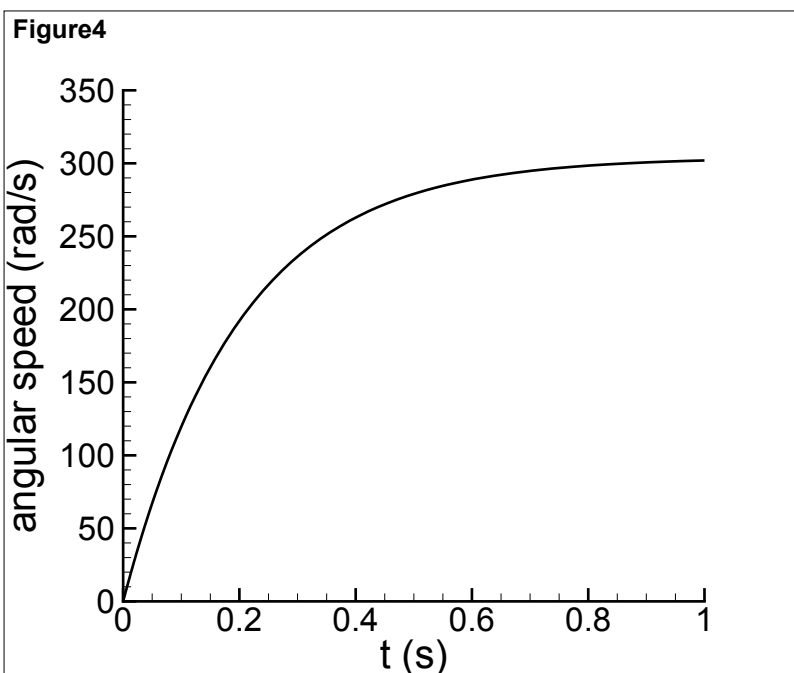


Figure5

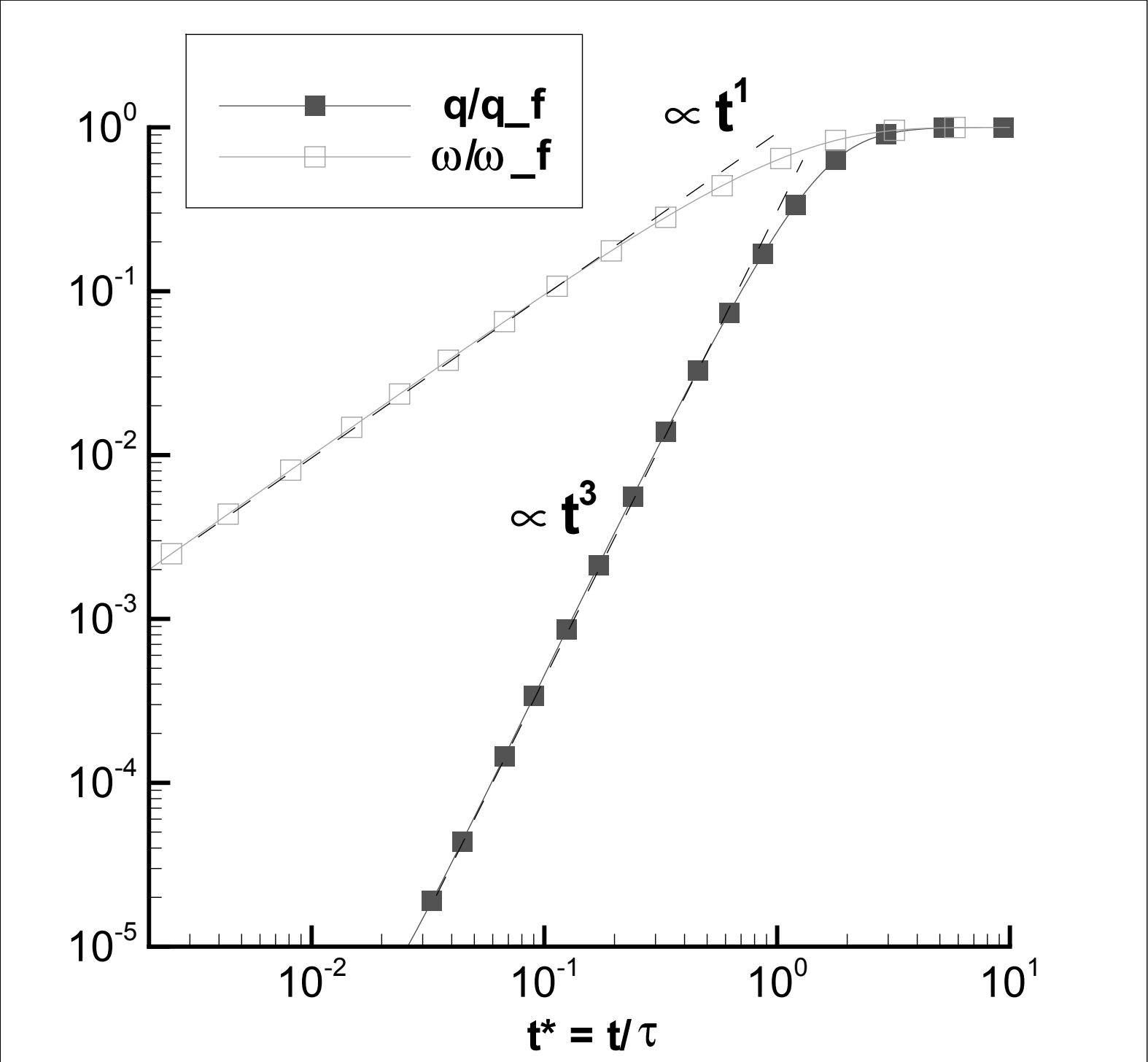


Figure6a

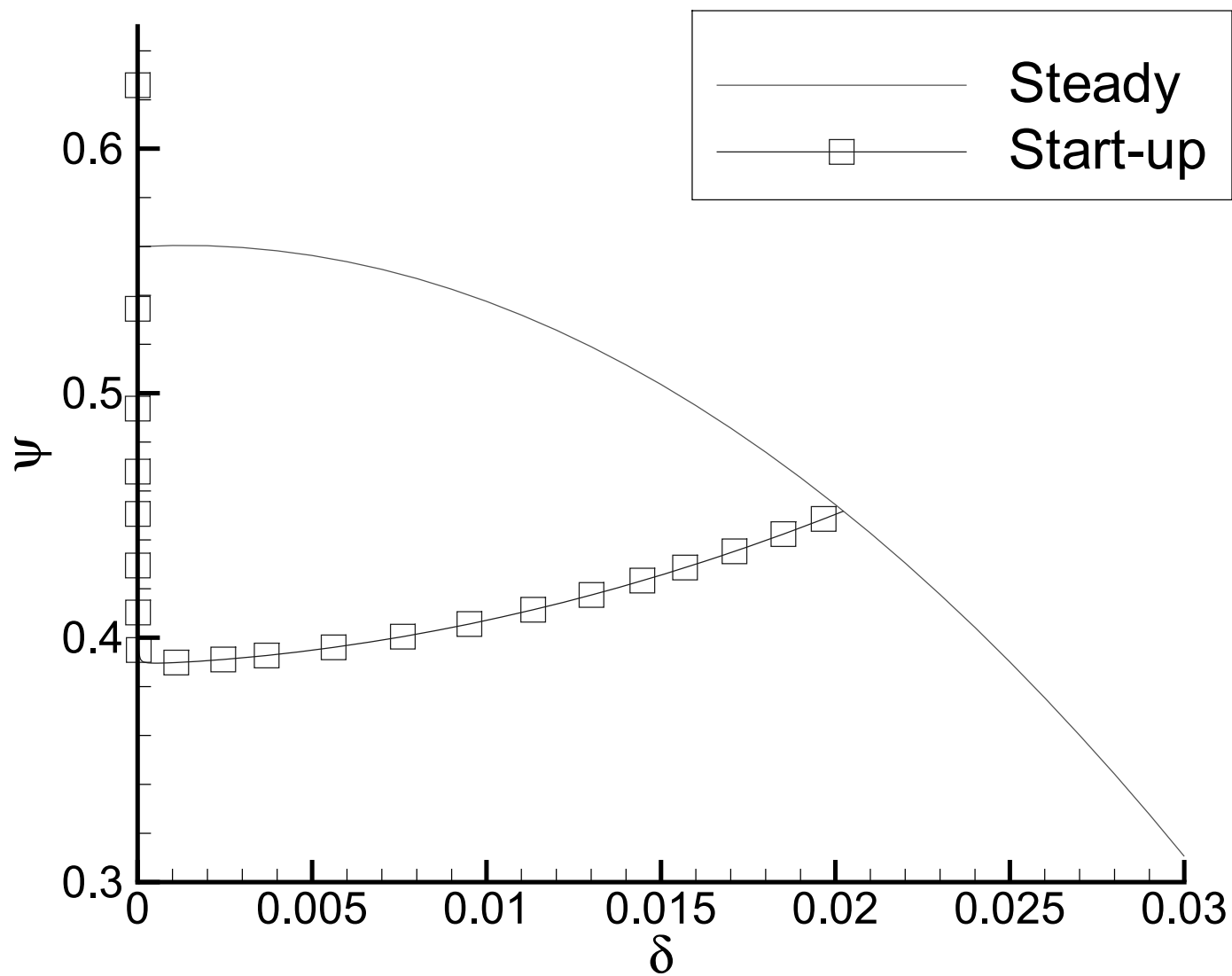


Figure6b

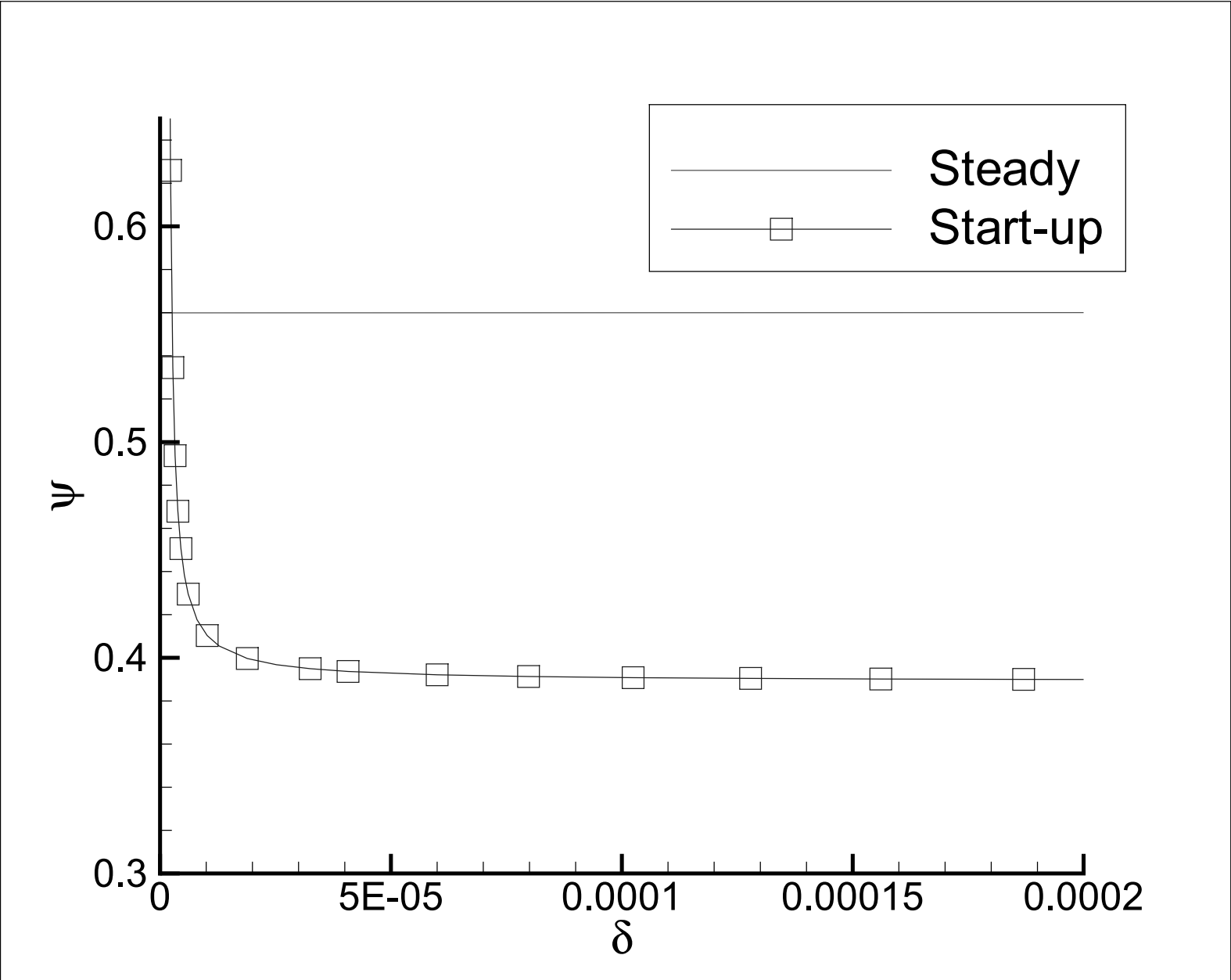


Figure7

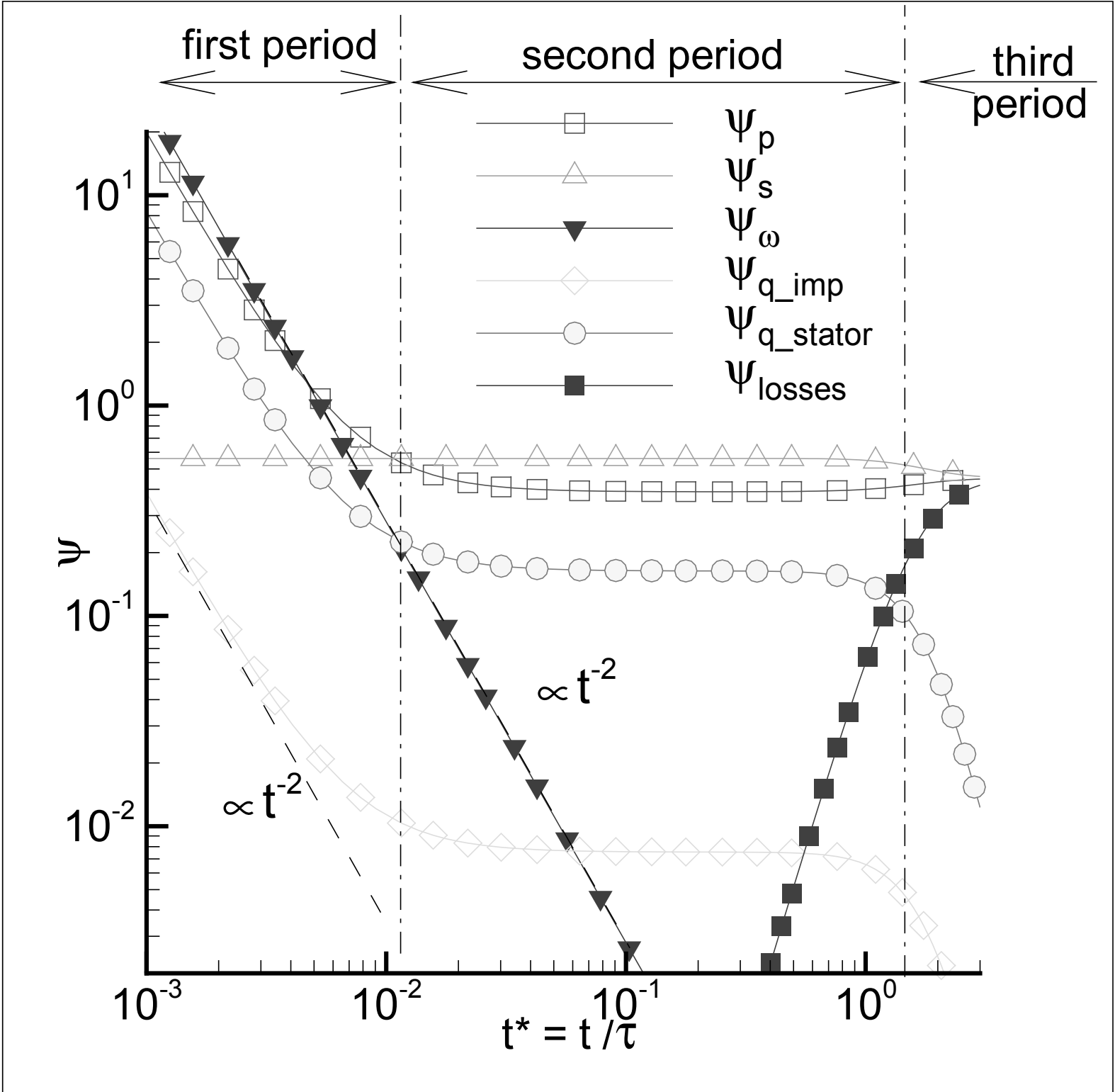


Figure8

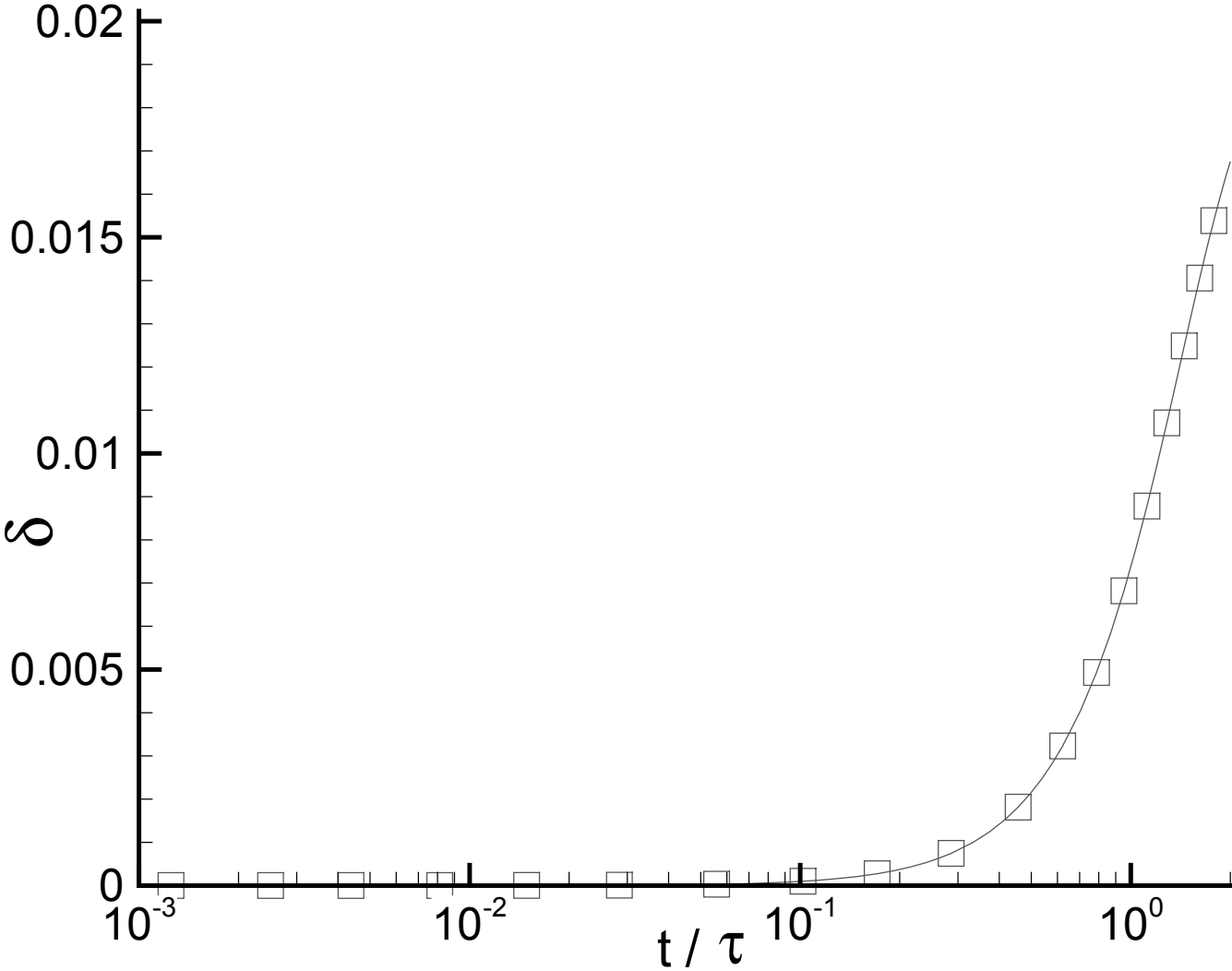


Figure9

